

---

## Design and research of red-blue confrontation training system based on virtual reality

---

Song Yong

Nanjing Police University,  
Nanjing, China  
Email: 112105@nfpc.edu.cn

Haili Yin\*

Nanjing Institute of Physical Education and Sports,  
Nanjing, China  
Email: yinhaili72@126.com  
\*Corresponding author

**Abstract:** In order to show the scene of military confrontation more truly and enhance the immersion of soldiers in confrontation, the behaviour generation of virtual soldiers is added. In order to solve the problem of red-blue confrontation system, this paper constructs a red-blue confrontation training system combined with virtual reality technology, simulates virtual soldiers with motion editing and motion redirection technology, uses motion redirection algorithm based on forward kinematics for kinematics simulation calculation, uses frame-by-frame solution method to process motion number, and uses surface model as collision detection model. Through simulation example images, it can be seen that the virtual reality technology proposed in this paper can realise interactive simulation of red-blue confrontation. At the same time, from the victory rate test of both sides of red-blue confrontation, it can be seen that the theoretical victory rate and the test victory rate are very close, so the red-blue confrontation training system based on virtual reality has obvious effect and can effectively improve the simulation effect of subsequent red-blue confrontation.

**Keywords:** virtual reality; red-blue confrontation; training; military.

**Reference** to this paper should be made as follows: Yong, S. and Yin, H. (2024) 'Design and research of red-blue confrontation training system based on virtual reality', *Int. J. Information and Communication Technology*, Vol. 25, No. 5, pp.1–17.

**Biographical notes:** Song Yong is a Master's student and graduated from Nanjing Sports College in 2003. He worked at the Special Police College of Nanjing Police University. His research directions police tactics, police combat, use of police equipment and equipment, police psychological and behavioural training, and field sports.

Haili Yin is a Professor in Nanjing Institute of Physical Education and Sports, His research area is traditional sports health theory and practice.

---

## **1 Introduction**

Traditional combat modelling and simulation method view describes military activities through mathematical modelling. Representative methods include analytical model based on Lanchester equation, statistical model based on Monte Carlo method and empirical model based on exponential method to describe combat effectiveness. The main characteristics of this kind of model are intuitive and easy to understand. It considers various quantifiable factors in the war process in detail, and describes the objective constraints of the factors considered on operational losses with simple analytical equations. This model has made some achievements in the process of describing mechanised warfare, but its application scenarios are based on many strict assumptions, which makes it difficult to meet the requirements of combat modelling and simulation under the background of modern information warfare system and network-centric warfare.

Modelling and simulation technology, as a virtual deduction method for the objective world, is widely used in various engineering fields and has a great promoting effect on social production. Virtual soldier behaviour generation refers to the autonomous and intelligent simulation of virtual soldier behaviour achieved through computers (Goecks et al., 2023). With the continuous development of computer generated forces (CGF) technology, virtual soldier behaviour generation has also been incorporated into CGF. The other part is the interaction between virtual soldiers and battlefield scenes in the AR battlefield (Hokianto and Fianty, 2022). The generation of virtual soldier behaviour in the AR battlefield can reduce the participation of combat personnel and weapons, thereby lowering the cost of adversarial training; On the other hand, virtual soldier behaviour is implemented by computers, and large-scale virtual soldiers are controlled by operators, which can enable virtual soldiers to perform set tactical actions and complete collaborative operations between virtual soldiers (Blacker et al., 2021).

Grimaila (2024) proposes a multi aircraft air combat adversarial evaluation system. This system is a computer simulation system that integrates actual measurement information and simulation information, with modern air combat models as the core. Binsch et al. (2021) developed an air combat training system. The system adopts full digital or semi physical simulation methods to train pilots to conduct virtual training on existing combat strategies, or to repeatedly practice and seek the best countermeasures for enemy aircraft in a certain combat strategy. The focus is on simulating the movement and trajectory generation of the target aircraft, and visualising the flight trajectory using software such as OpenGL.

Mendi et al. (2021) addresses the issue of neglecting the interrelationships between artillery and other branches in artillery combat simulation, and establishes a combat simulation system based on artillery units. This system conducts simulation research on artillery platform level/aggregation level entities, with a focus on simulating the combat actions of artillery units in joint campaigns.

The purpose of simulation training is to simulate different battlefield situations, so that participants can accumulate experience through simulation training to improve their ability to respond on real battlefields. If there is a significant difference between the training process and the actual situation, the training effect will be greatly reduced. In order to ensure the authenticity of training, the most important point is that virtual and real forces can perceive each other, and interaction between virtual and real soldiers is

required. Virtual soldiers also need to be able to make corresponding responses according to the battlefield situation (Çelenk and Tokan, 2022).

In order to enable soldiers to cope with various combat environments in actual combat and adopt corresponding response plans in different situations, it is required that the system can simulate different situations during training and freely add different components according to training needs. In this way, simulation control personnel can freely add defensive fortifications, weapons and equipment, as well as virtual combat forces according to training needs (Singh et al., 2023).

In order to analyse and summarise the training process after each simulation training, it is necessary for the training system to record the training data during training and use the recorded data to restore and replay the entire training process after the simulation is completed (Lee et al., 2020).

Qays et al. (2020) uses artificial intelligence to improve the firepower allocation algorithm, but when solving firepower allocation problems, it still relies on gradient descent method and is prone to falling into local optima. Oh et al. (2021) designed the firepower allocation algorithm as a parallelised algorithm, and its optimised algorithm can greatly accelerate computational efficiency and obtain a relatively optimal allocation scheme. Wang et al. (2021) proposed a multi kill vehicle firepower allocation algorithm based on adjusted genetic algorithm. This algorithm automatically adjusts the crossover probability and mutation rate of the population, accelerates the convergence speed of the algorithm, improves the detection ability mutation rate of the algorithm, and effectively solves the problem of interceptor task allocation. Deng et al. (2020) proposed a variable parameter genetic algorithm and applied it to the firepower optimisation allocation problem of air defence units. Real number encoding was used to construct chromosomes to create the original population, calculate fitness, check the original population, operate inheritance algorithm operators, improve election, crossover, mutation and other operations. Etewa et al. (2023) proposed a target optimisation allocation model based on shooting advantage for the characteristics of target allocation in air defence operations, and provided a cyclic reduction algorithm for solving the model from the perspective of engineering applications. This algorithm is simple and convenient, and has high engineering application value. Gaikwad et al. (2020) combines deep learning technology with auxiliary decision-making, and proposes intelligent methods for thinking and decision-making in battlefield knowledge extraction, situational understanding and cognition, combat intention prediction, self confrontation simulation, human-machine interaction, etc. It explores the construction of models for three main problems: battlefield target recognition, combat intention prediction, and simulated adversarial games. Abdolhosseinzadeh et al. (2022) combines simulated annealing algorithm with genetic algorithm to establish a target allocation model with the goal of maximising interception success under various constraints. A global optimisation method for solving target allocation is proposed, and experiments have shown that this algorithm has better convergence and optimisation effects than genetic algorithm, providing ideas for complex multi weapon target allocation problems in missile defence. Dorn et al. (2020) proposes to combine simulation cloning technology with command and control assisted decision-making systems, and designs a command and control assisted decision-making system based on simulation cloning. By using decision point-based analysis tree method, the operational efficiency of traditional command and control assisted decision-making systems is improved, providing time guarantee for the application of simulation systems

in command and control systems. Stein et al. (2023) focuses on the firepower allocation problem of surface targets, and uses chaotic particle swarm optimisation algorithm to solve the firepower allocation scheme based on the optimal aiming point, verifying the superiority of chaotic particle swarm algorithm in terms of search accuracy and search efficiency when used for firepower allocation problem solving

In order to improve the simulation effect of red-blue confrontation training, this paper constructs a red-blue confrontation training system combined with virtual reality technology, generates a virtual avatar of a real soldier in augmented reality environment, and makes the virtual avatar synchronise with the actions of the real soldier. Then, combined with digital virtual technology, the simulation research is carried out to provide reference for the improvement of the simulation effect of the follow-up red-blue confrontation scene.

## 2 Virtual and real perception and interaction system design

In order to realise the perception of virtual soldiers to real soldiers, it is necessary to generate a virtual avatar of real soldiers in augmented reality environment, and make the virtual avatar synchronise with the actions of real soldiers, so it is necessary to use motion editing and motion redirection technology.

The attitude of the joint node can be calculated from the attitude of the parent node, and the parent node can traverse upward step by step until the root node is known, so the attitude of the joint node can be calculated from the root node. As shown in Figure 1, the attitude of the joint node  $P_2$  relative to the root node  $P_0$  in the figure is (Varol Arısoy and Küçükşille, 2021):

$$M_{2 \rightarrow 0} = M_{2 \rightarrow 1} M_{1 \rightarrow 0} \quad (1)$$

Among them,  $M_{i \rightarrow j}$  is the attitude of joint node  $P_i$  relative to joint node  $P_j$ . Similarly, the attitude of joint node  $P_5$  relative to root node  $P_0$  is:

$$M_{5 \rightarrow 0} = M_{5 \rightarrow 4} M_{4 \rightarrow 3} M_{3 \rightarrow 0} \quad (2)$$

The attitude of any joint  $P_i$  relative to the root node  $P_0$  is:

$$M_{i \rightarrow 0} = \prod_{j=0}^{i-1} M_{j \rightarrow p(j)} \quad (3)$$

Among them,  $P(i)$  is the number of the parent node  $P_i$ . Therefore, the attitude of any joint  $P_i$  relative to the global coordinates is:

$$M_{i \rightarrow M} = M_{i \rightarrow 0} M_{0 \rightarrow M} \quad (4)$$

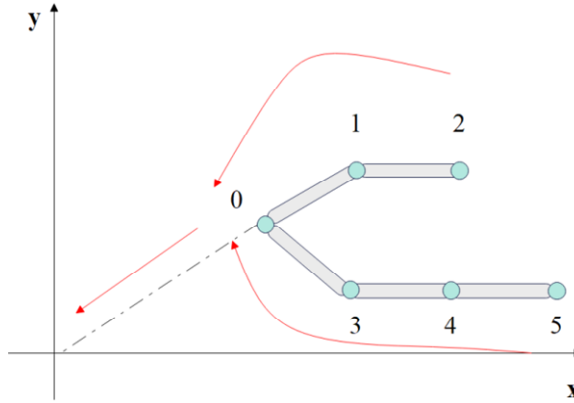
Therefore, the transformation of any joint  $P_i$  into the world coordinate system can be written as:

$$M_{i \rightarrow W} = M_{i \rightarrow M} M_{M \rightarrow W} \quad (5)$$

Because the joint length of the source skeleton and the target skeleton may be different, and the position of the root node does not change compared with the source skeleton, the

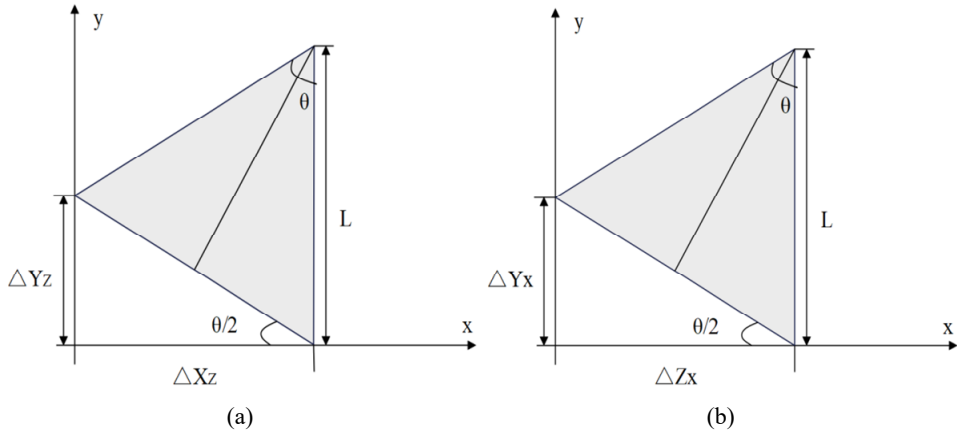
avatar may penetrate or hang. In order to solve this phenomenon, it is necessary to introduce displacement compensation algorithm to solve this problem.

**Figure 1** Space model of joint node (see online version for colours)



When creating the skeleton of the avatar, in order to be consistent with the topology of the skeleton of the motion capture system, the far point of the world coordinate system is generally located at the root node of the avatar skeleton. However, when the human body moves, the origin of the world coordinate system is the foot, which will lead to the shift of the lower limb position. The set relationship of lower limb movement is shown in Figure 2 (Stein et al., 2022).

**Figure 2** Lower limb rotation, (a) rotate about the x-axis (b) rotate about the z-axis



If the length of the leg skeleton of the virtual avatar is set as  $L$ , when the root node is displaced and the leg joint node is not displaced, the displacement compensation of the leg skeleton rotating along the  $x$ -axis is as follows (Spiering et al., 2021):

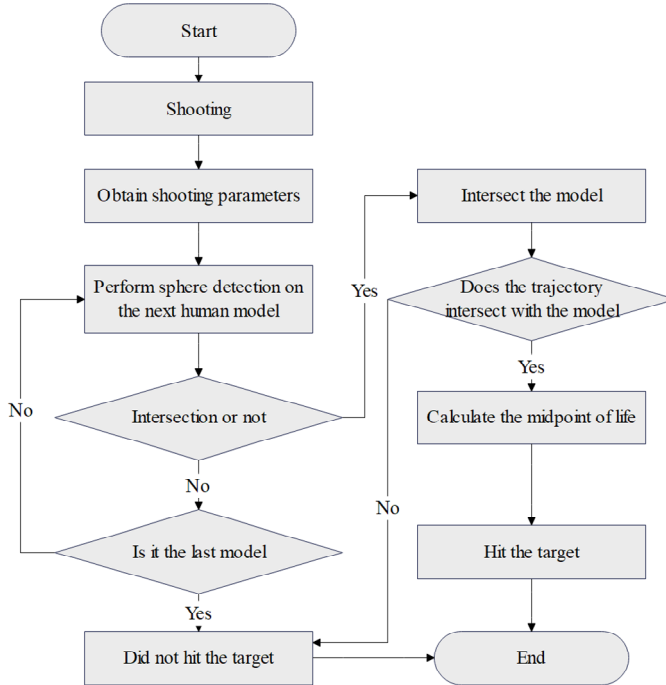
$$\begin{cases} \Delta Z_x = L \times \sin \theta \\ \Delta Y_x = 2L \times \left( \sin \frac{\theta}{2} \right)^2 \end{cases} \quad (6)$$

The displacement compensation for rotation along the  $z$ -axis is:

$$\begin{cases} \Delta X_z = L \times \sin \theta \\ \Delta Y_z = 2L \times \left( \sin \frac{\theta}{2} \right)^2 \end{cases} \quad (7)$$

When displacement compensation is added to the coordinates of the root node, the phenomenon of suspended puncture caused by the change of the root node can be eliminated.

**Figure 3** Schematic diagram of hit determination flow



Collision objects in virtual environment can be divided into surface model and volume model. Among them, surface model is defined by boundary, and volume model is defined by volume element. According to whether the object model will deform after collision, the surface model can be divided into rigid body model and non-rigid body model. According to the surface shape of the model, rigid body models can be divided into curved surface models and non-curved surface models.

In order to study the collision model, it is necessary to establish the mathematical model of collision. Because it is relatively easy to establish the mathematical model of surface model, the surface model is used as the collision detection model in this paper. The current collision detection technology mainly adopts three bounding box mathematical models: bounding ball AABB and OBB. Because the collision detection method using bounding ball is simple and time-consuming this paper adopts sphere detection.

When the system determines the hit, it will first detect the bounding ball of all the virtual avatar models in the system in turn. If it detects that a certain virtual avatar model intersects with the trajectory, it will accurately intersect the virtual avatar model with the trajectory to determine whether it hits or not. The specific process of hit determination is shown in Figure 3 (Linssen et al., 2022).

The mathematical model of spherical collision detection is simple, and whether collision occurs can be judged by judging the distance between spherical centres. When the distance between the centres of two balls is greater than the sum of radii, the spheres do not collide. When the distance between the centres of two spheres is less than or equal to the sum of radii, the principle of collision between spheres is shown in Figure 4. Because of the short range of the weapon used in this system, the trajectory can be approximated as a ray. Therefore, this paper adopts the way of intersection between ray and sphere to judge the hit. Figure 5 is a schematic diagram of the intersection of ray spheres in a two-dimensional plane. If we set the endpoint coordinate of the endpoint  $P$  of ray  $PA$  as  $p_0(x_0, y_0)$ , the direction vector as  $u(\theta, \varphi)$ , the centre coordinate of circle  $O$  as  $O(x_o, y_o)$  and the radius as  $r$ , then the equation of ray  $AP$  is (Qu et al., 2020):

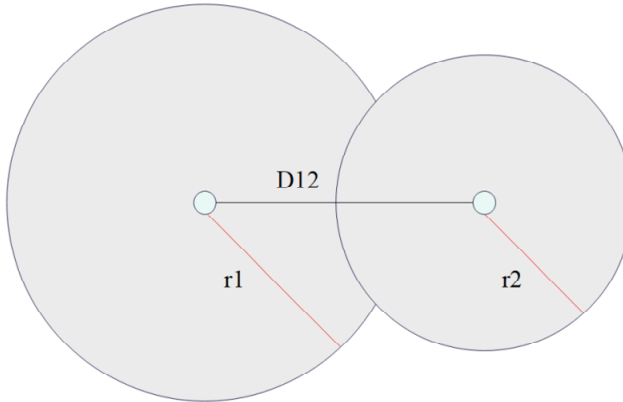
$$p(\lambda) = p_0 + \lambda u \quad (8)$$

When  $p(\lambda)$  is brought into the circle  $O$ , we can get:

$$\|p_0 + \lambda u - O\| - r = 0 \quad (9)$$

According to the intersection point theorem of ray and circle, when there is a real solution greater than or equal to zero in equation (9), the intersection of ray and circle can be judged. In three-dimensional space, the judgment condition is still valid.

**Figure 4** Schematic diagram of sphere collision (see online version for colours)



Due to the physiological limitations of human body, human joints will be constrained by some conditions, including joint length constraint and joint Euler angle constraint. Among them, joint length constraint refers to the bone length between two joints. For example, the length constraint between knee joint and ankle joint is the length of human calf bone, which cannot be changed during exercise. Joint Euler angle constraint means that the rotation of human joint is constrained. According to the different human body

parts where the joint is located, the rotation range of each joint is also different. Table 1 shows the value range of Euler angle of hand-foot joint.

**Figure 5** Schematic diagram of ray sphere intersection (see online version for colours)

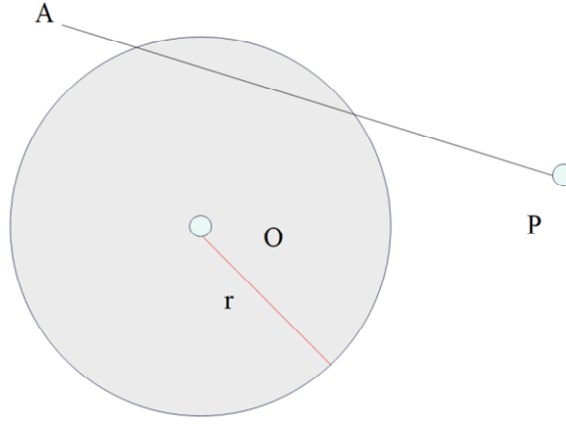


**Table 1** Value range of Euler angle of human hand-foot joint

	Coordinate axis	Maximum (°)	Minimum (°)
Left hand	X	90	-90
	Z	20	-20
Right hand	X	90	-90
	Z	20	-20
Left foot	Y	20	-20
	Z	20	-20
Right foot	Y	20	-20
	Z	20	-20

Joint editing considers three factors: human body orientation, contact point information of end joint and displacement of root joint.

- 1 For the acquired human pose sequence, the first frame points to the positive half axis of  $z$ . We remember that the joint coordinates of pelvis, left pelvis, left ankle and right ankle are  $p_h, p_{lh}, p_{la}, p_{ra}$ , and  $p_m$  represents the centre coordinates of left and right ankles, the orientation of human body is expressed by vector  $\vec{n}$ ,  $M$  represents the rotation matrix from rotating  $\vec{n}$  to the positive half axis of  $z$  axis, and  $p'_i$  represents the joint coordinates after  $p_i$  changes.

$$\begin{aligned}
 p_m &= (p_{lf} + p_{rf})/2 \\
 \vec{n} &= \overrightarrow{p_h p_m} \times \overrightarrow{p_h p_{lh}} \\
 p'_i &= M \cdot p_i
 \end{aligned} \tag{10}$$

- 2 For the joint of hand and foot, besides meeting the Euler angle constraint in Table 1, it is necessary to ensure that the foothold is on  $xz$  plane. When both hands hold a



gun, the distance between the left and right hands is the distance between the handle of the gun and the dragging hand, which is a fixed value. We remember that the coordinates of the joint points of left hand, right hand, left wrist and left foot are  $p_{lhand}$ ,  $p_{rhand}$ ,  $p_{lwrist}$  and  $p_{lfoot}$ , and  $L_{hbone}$  and  $L_{fbone}$  represent the length of palm and foot bones, and  $L_{gun}$  represents the distance between the handle of the gun and the dragging hand.

$$\begin{aligned} |p_{la} p_{lfoot}| &= L_{fbone} \\ |p_{lwrist} p_{lhand}| &= L_{hbone} \\ |p_{lhand} p_{rhand}| &= L_{gun} \end{aligned} \quad (11)$$

- 3 The root joint displacement of the key frame is calculated according to the human body displacement estimation ( $\Delta x$ ,  $\Delta y$ ,  $\Delta z$ ) in the video:

$$\begin{aligned} x'_i &= x_i + \Delta x \\ y'_i &= y_i + \Delta y \\ z'_i &= z_i + \Delta z \end{aligned} \quad (12)$$

The whole basic action sequence of soldiers is obtained by local key frame interpolation algorithm. For the root joint, it only has spatial displacement change, and general linear interpolation is adopted. For two adjacent frames  $t_1$  and  $t_2$ , the root joint positions are  $p_1$  and  $p_2$  ( $t_1 < t < t_2$ ) respectively, so the linear interpolation between them is:

$$p_t = \frac{t_2 - t}{t_2 - t_1} p_1 + \left(1 - \frac{t_2 - t}{t_2 - t_1}\right) p_2 \quad (13)$$

Except the root node, all the other joints are about the rotation of the parent node, and the quaternion spherical linear interpolation is adopted. Quaternion spherical interpolation refers to the interpolation on the unit sphere. For the unit quaternions  $q_1$  and  $q_2$ ,  $Slerp(q_1, q_2, t)$  represents the spherical interpolation of  $q_1$  and  $q_2$  (Dorn and Dawson, 2021):

$$\begin{aligned} \theta &= \arccos(q_1 \times q_2) \\ Slerp(q_1, q_2, t) &= \frac{\sin(1-t)\theta}{\sin \theta} q_1 + \frac{\sin t\theta}{\sin \theta} q_2, t \in [0, 1] \end{aligned} \quad (14)$$

$\theta$  represents the angle of rotation around the unit vector. For all key frames, according to the frame number of key frames in the attitude sequence, the number of frames to be inserted is calculated. For example, key frame number 1 is the first frame in the sequence, key frame number 2 is the 15th frame. Then, a complete action sequence is generated by pairwise interpolation in order to ensure that the interpolated action sequence has the same frame number as the video.

### 3 System design

The virtual-real soldier confrontation training system designed in this paper is mainly composed of positioning system, motion capture system, computer generated soldier system, virtual-real perception and interaction system and distributed virtual-real perception platform. The overall architecture of the system and the relationships among

its parts are shown in Figure 6. Among them, the research objects of this paper are distributed virtual-real perception platform, motion capture system and virtual-real perception and interaction system.

**Figure 6** Schematic diagram of the overall architecture of the system

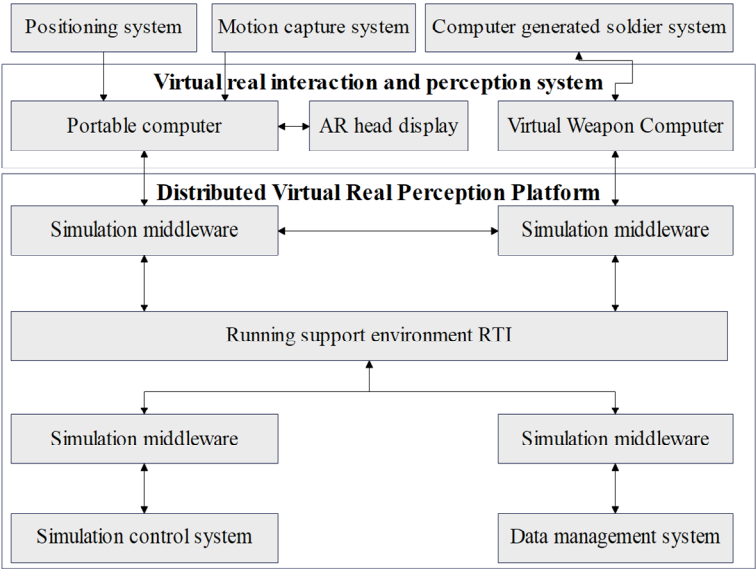
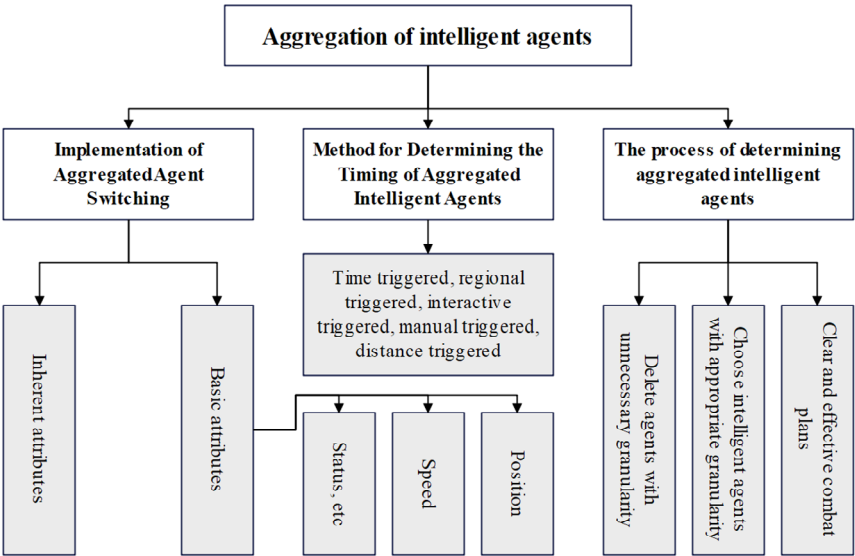


**Figure 7** System flow chart of agent aggregation

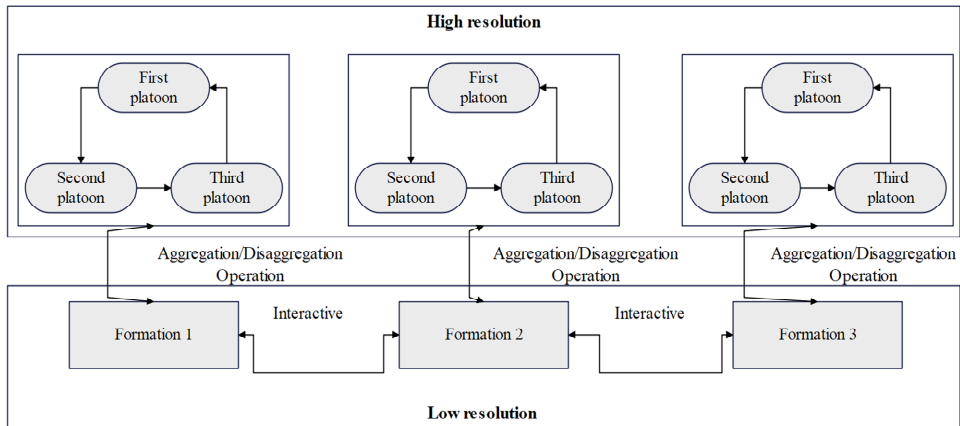


The output process of macro instruction refers to the instruction obtained after hierarchical task network planning, which is sent to each agent. In the process of combat simulation, in order to achieve the combat goal, military personnel need to solve three

problems in realising model aggregation method: the determination of aggregation agents, that is, which agents to choose for aggregation, the determination of aggregation opportunity, that is, the determination of aggregation opportunity, that is, the timing of model aggregation, including a series of aggregation mechanisms and artificial trigger mechanisms formulated by the system, and the realisation of aggregation agent switching, that is, the problem of the mapping of entity attributes and the improvement of data in the process of resolution change. Therefore, for each problem, it is necessary to formulate a characteristic process. Figure 7 shows the system flow of agent aggregation.

First of all, it is necessary to check the agents with different resolutions of participating combat entities as a whole, clarify the interaction relationship among agents, avoid the problem of cross-resolution interaction, and delete unnecessary unused resolution agents. As shown in Figure 8, the same entity has a hierarchical high-low resolution model, and the interaction of each agent needs to be aggregated/de-aggregated to reach the same level of the entity before it is feasible.

**Figure 8** Schematic diagram of interaction between high and low resolution agents of the same entity with hierarchy



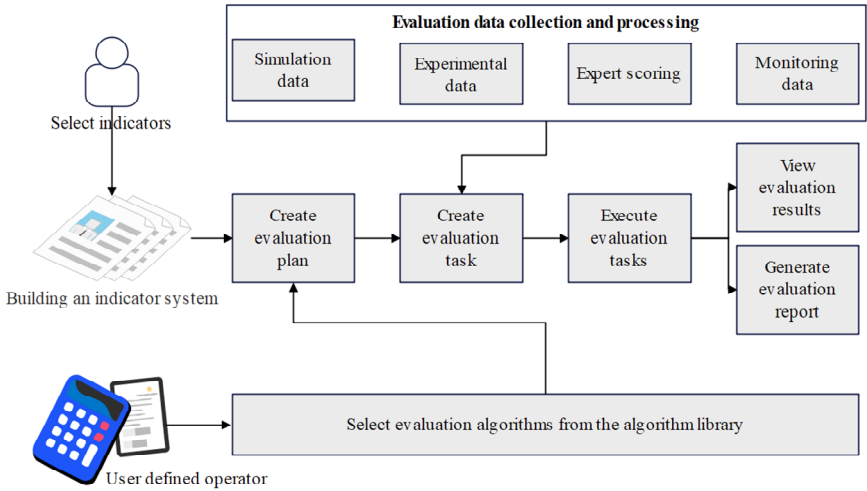
## 4 Experimental study

Because the models contained in the simulation system are huge in order of magnitude and complex in function, it is difficult to fully understand all the models, but it is necessary to choose the aggregation model according to the opinions of all parties on the basis of understanding the combat objectives. Therefore, the contradiction between them is easy to cause a large number of errors and affect the simulation deduction results, which is very time-consuming and laborious.

As shown in Figure 9, the evaluation system selects the evaluation index, constructs the index system, selects the evaluation algorithm from the algorithm library and creates the evaluation scheme. During the evaluation data collection and processing, simulation data collection, test data, expert scoring and monitoring data are needed, and then the evaluation task is created. After executing the evaluation task, the evaluation result is

viewed, and the evaluation report is generated and saved for the next analysis and viewing

**Figure 9** Structure diagram of evaluation system (see online version for colours)



All the experimental environment configurations in this paper are shown in Table 2.

**Table 2** Software and hardware configuration of experimental environment

Software and hardware names	Model
Processor	Core i7-14700F
Graphics card	NVIDIA RTX 3080
Video memory	12
Memory	32
System environment	Windows 11 version 22H2

For virtual soldiers in AR battlefield, the status of hands and feet cannot be ignored. For example, when holding a gun, hands and guns, feet and the ground need seamless contact, so that the generated actions are more real and reasonable, and the immersion of participating soldiers is enhanced.

Figure 10 shows the first frame of a soldier squatting forward with a gun. Compared with the left picture, the right picture considers the contact between soldiers and the ground, that is, xz plane, bone length, and Euler constraint relationship between toes and ankles during advancement, and adds toe joints. Moreover, the right figure considers the soldier's gun holding posture, bone length, and Euler restraint between hand and ankle, and adds hand joints.

The joints extracted from the video will appear jitter. As shown in Figure 11, elbow and knee represent the left elbow and knee before processing, and elbow \* and knee \* represent the left elbow and knee after interpolation through key frame extraction.

**Figure 10** The first frame of a soldier squatting forward with a gun, (a) no hand foot end joint (b) having joints at the ends of hands and feet (see online version for colours)

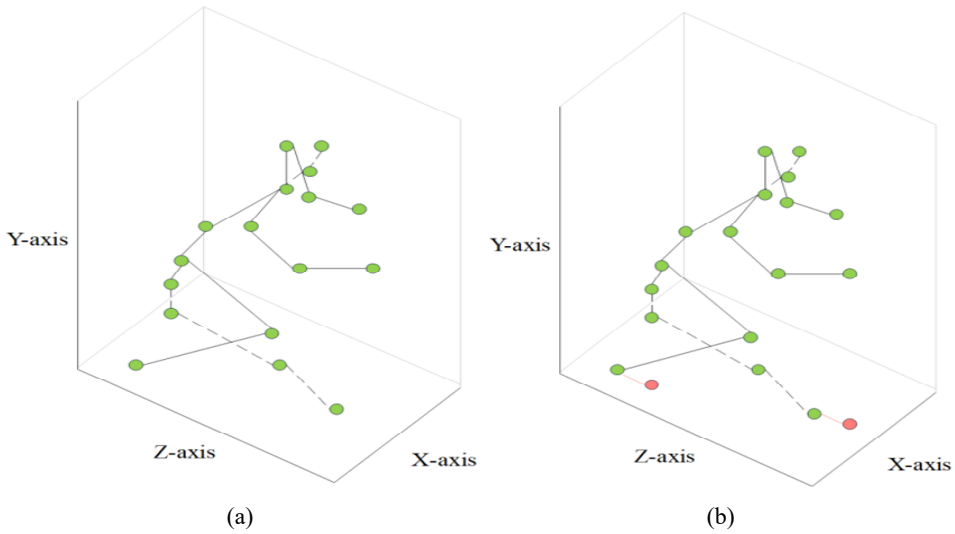
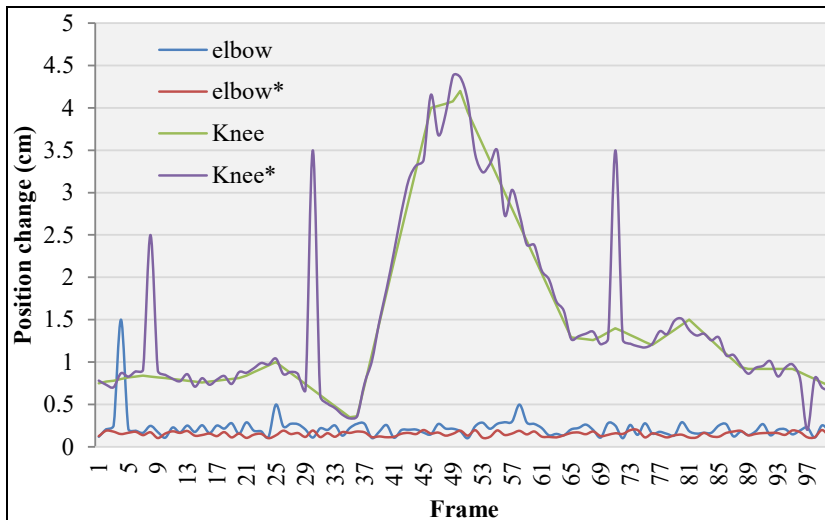


**Figure 11** Position changes of left knee and left elbow joints (see online version for colours)



It can be seen from the figure that the elbow changes relatively little, but the knee changes greatly, which is in line with people's intuitive feelings. Compared with knee\*, knee has sudden changes in frames 7, 30, 55, 72 and 97, which means that the joint position of action sequence changes violently at these frames, that is, jitter appears. These jitter frames appear for the following two reasons. On the one hand, the reason is that the quality of soldiers' action video obtained from the Internet is not high, and the clarity affects the 2D joint position obtained by Alphapose. On the other hand, the sudden change of video shooting angle will affect the output result of 3D attitude extraction network. Figure 12 shows an example of key frame extraction.

**Figure 12** Key frame extraction of soldier squatting action, (a) keyframes without hand and foot joints (b) adding keyframes to hand and foot joints (see online version for colours)

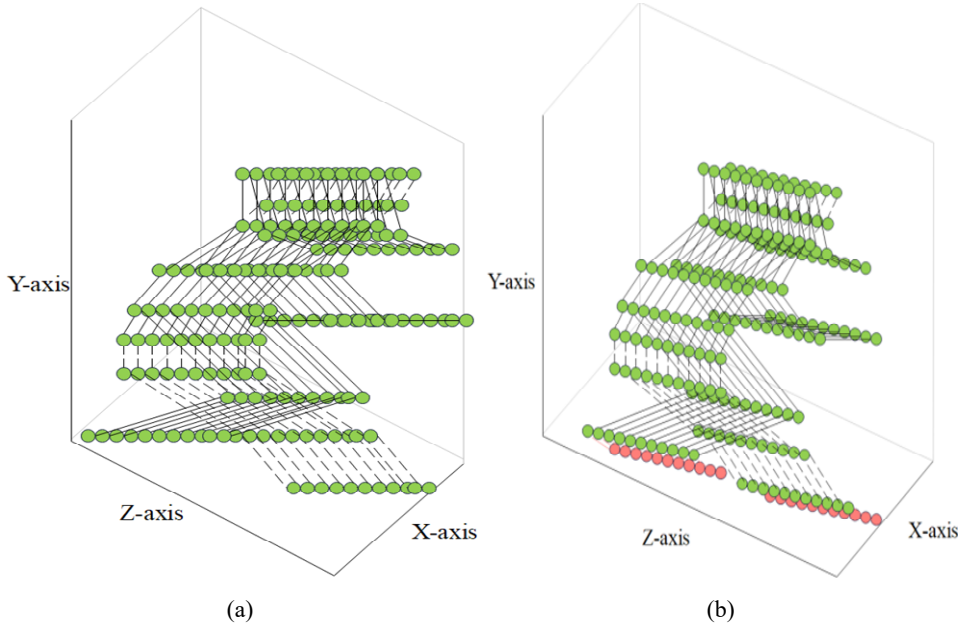


Figure 13 shows the scene simulation diagram of red-blue confrontation.

**Figure 13** Scene simulation diagram of red-blue confrontation (see online version for colours)

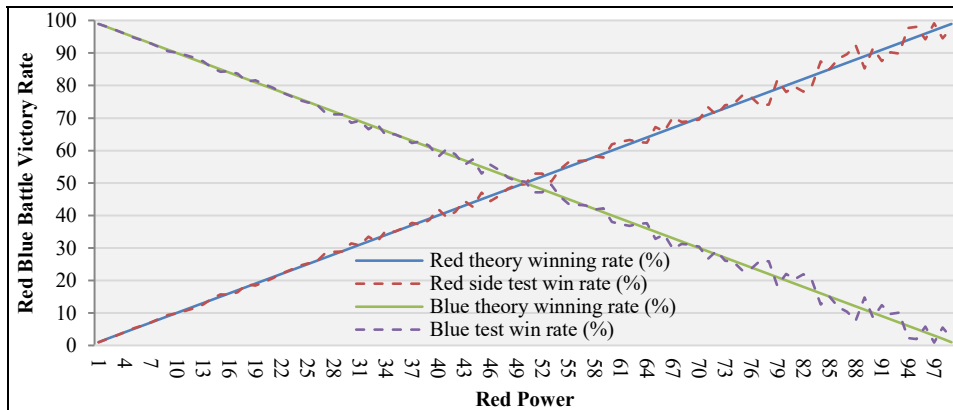


Based on the above analysis, this paper sets the strength distribution of red and blue in [1, 99]. For the convenience of the test, the sum of red and blue strength is set to 100, that is, the strength of red and blue is 50 and the strength of blue is 50. As long as the final simulation of the winning rate of both sides is 50%, it proves that the system constructed

in this paper is effective. When the strength of red and blue is 10% and 90%, the winning rate of both sides is 10% and 90%, which can get the theoretical winning rate of red and blue, and can be compared with the test winning rate. If the test winning rate is close to the theoretical winning rate, it can verify that the system is effective.

On the basis of this experimental condition, the simulation experiment is carried out. Because the sum of red and blue strength is set to 100 in this paper, the blue strength can be obtained as long as the red strength is obtained, and the simulation test results shown in Figure 14 are obtained.

**Figure 14** Simulation test results of red-blue confrontation (see online version for colours)



As shown in Figure 14, from the winning rate diagram of both sides of red-blue confrontation, the theoretical winning rate is very close to the test winning rate. Therefore, the red-blue confrontation training system based on virtual reality proposed in this paper has obvious effect, which can effectively improve the simulation effect of subsequent red-blue confrontation.

## 5 Conclusions

Because of its unique advantages in military training exercises, such as scientificness, economy, antagonism, intuition, interactivity and real-time, virtual battlefield solves the shortcomings of conventional military training, such as huge cost and poor security, and provides a more effective way for military strategic, campaign and tactical drills, which greatly improves the quality of military training. As a new simulation solution, the combination of distributed interactive simulation and virtual reality has the characteristics of high efficiency, economy, security and intuition. With the continuous improvement of computer graphics, visualisation technology, simulation technology, distributed technology and computer hardware performance, it will be widely used. This paper presents a red-blue confrontation training system based on virtual reality, and the performance of the system is verified by simulation experiments. Through the simulation examples, it can be seen that the virtual reality technology proposed in this paper can realise the interactive simulation of red-blue confrontation. At the same time, through the victory simulation, it can be seen that the red-blue confrontation training system based on

virtual reality proposed in this paper has obvious effect, which can effectively improve the simulation effect of subsequent red-blue confrontation.

## References

- Abdolhosseinzadeh, A., Akhlaghi, T. and Katebi, H. (2022) 'Effect of a row of soldier piles on the settlement of adjacent buildings due to tunnelling: numerical study', *International Journal of Geotechnical Engineering*, Vol. 16, No. 5, pp.616–631.
- Binsch, O., Bottenheft, C., Landman, A., Roijendijk, L. and Vermetten, E.H. (2021) 'Testing the applicability of a virtual reality simulation platform for stress training of first responders', *Military Psychology*, Vol. 33, No. 3, pp.182–196.
- Blacker, K.J., Pettijohn, K.A., Roush, G. and Biggs, A.T. (2021) 'Measuring lethal force performance in the lab: the effects of simulator realism and participant experience', *Human Factors*, Vol. 63, No. 7, pp.1141–1155.
- Çelenk, E. and Tokan, N.T. (2022) 'All-textile on-body antenna for military applications', *IEEE Antennas and Wireless Propagation Letters*, Vol. 21, No. 5, pp.1065–1069.
- Deng, P.Y., Qiu, X.Y., Tang, Z., Zhang, W.M., Zhu, L.M., Ren, H. and Sheng, R.S. (2020) 'Detecting fatigue status of pilots based on deep learning network using EEG signals', *IEEE Transactions on Cognitive and Developmental Systems*, Vol. 13, No. 3, pp.575–585.
- Dorn, A.W. and Dawson, P.F. (2021) 'Simulating peace operations: new digital possibilities for training and public education', *Simulation & Gaming*, Vol. 52, No. 2, pp.226–242.
- Dorn, A.W., Webb, S. and Pâquet, S. (2020) 'From wargaming to peacegaming: digital simulations with peacekeeper roles needed', *International Peacekeeper*, Vol. 27, No. 2, pp.289–310.
- Etewa, M., Safwat, E., Abozied, M.A.H. and El-Khatib, M.M. (2023) 'Modeling and systematic investigation of a small-scale propeller selection', *Journal of Engineering Science and Military Technologies*, Vol. 7, No. 1, pp.15–21.
- Gaikwad, N.B., Ugale, H., Keskar, A. and Shivaprakash, N.C. (2020) 'The internet-of-battlefield-things (IoBT)-based enemy localization using soldiers location and gunshot direction', *IEEE Internet of Things Journal*, Vol. 7, No. 12, pp.11725–11734.
- Goecks, V.G., Waytowich, N., Asher, D.E., Jun Park, S., Mittrick, M., Richardson, J. and Kott, A. (2023) 'On games and simulators as a platform for development of artificial intelligence for command and control', *The Journal of Defense Modeling and Simulation*, Vol. 20, No. 4, pp.495–508.
- Grimaila, M.R. (2024) 'Modeling and simulation in graduate military education', *The Journal of Defense Modeling and Simulation*, Vol. 21, No. 1, pp.3–4.
- Hokianto, W. and Fianty, M.I. (2022) 'Analyzing level of international humanitarian law knowledge and its compliance through military simulation game', *Ultimatics: Jurnal Teknik Informatika*, Vol. 14, No. 2, pp.111–118.
- Lee, S., Youn, J. and Jung, B.C. (2020) 'A cooperative phase-steering technique in spectrum sharing-based military mobile ad hoc networks', *ICT Express*, Vol. 6, No. 2, pp.83–86.
- Linssen, L., Landman, A., van Baardewijk, J.U., Bottenheft, C. and Binsch, O. (2022) 'Using accelerometry and heart rate data for real-time monitoring of soldiers' stress in a dynamic military virtual reality scenario', *Multimedia Tools and Applications*, Vol. 81, No. 17, pp.24739–24756.
- Mendi, A.F., Erol, T. and Doğan, D. (2021) 'Digital twin in the military field', *IEEE Internet Computing*, Vol. 26, No. 5, pp.33–40.
- Oh, H.S., Kim, D. and Lee, S. (2021) 'Review on the quality attributes of an integrated simulation software for weapon systems', *Journal of the Korea Institute of Military Science and Technology*, Vol. 24, No. 4, pp.408–417.



- Qays, H.M., Jumaa, B.A. and Salman, A.D. (2020) 'Design and implementation of autonomous quadcopter using SITL simulator', *IRAQI Journal of Computers, Communications, Control and Systems Engineering*, Vol. 20, No. 1, pp.1–15.
- Qu, H., Yu, L.J., Wu, J.T., Liu, G., Liu, S.H., Teng, P. and Zhao, Y. (2020) 'Spine system changes in soldiers after load carriage training in a plateau environment: a prediction model research', *Military Medical Research*, Vol. 7, No. 1, pp.1–11.
- Singh, S., Manju, Malik, A. and Singh, P.K. (2023) 'A threshold-based energy efficient military surveillance system using heterogeneous wireless sensor networks', *Soft Computing*, Vol. 27, No. 2, pp.1163–1176.
- Spiering, B.A., Walker, L.A., Larcom, K., Frykman, P.N., Allison, S.C. and Sharp, M.A. (2021) 'Predicting soldier task performance from physical fitness tests: reliability and construct validity of a soldier task test battery', *Journal of Strength and Conditioning Research*, Vol. 35, No. 10, pp.2749–2755.
- Stein, J.A., Hepler, T.C., DeBlauw, J.A., Beattie, C.M., Beshirs, C.D., Holte, K.M. and Farina, E.K. (2023) 'Anthropometrics and body composition predict performance during a simulated direct-fire engagement', *Ergonomics*, Vol. 66, No. 7, pp.904–915.
- Stein, J.A., Hepler, T.C., DeBlauw, J.A., Beattie, C.M., Beshirs, C.D., Holte, K.M. and Heinrich, K.M. (2022) 'Lower-body muscular power and exercise tolerance predict susceptibility to enemy fire during a tactical combat movement simulation', *Ergonomics*, Vol. 65, No. 9, pp.1245–1255.
- Varol Arisoy, M. and Küçüksille, E.U. (2021) 'Landmine detection training simulation using virtual reality technology', *Virtual Reality*, Vol. 25, No. 2, pp.461–490.
- Wang, D., Zhang, Z., Zhang, M., Fu, M., Li, J., Cai, S. and Chen, X. (2021) 'The role of digital twin in optical communication: fault management, hardware configuration, and transmission simulation', *IEEE Communications Magazine*, Vol. 59, No. 1, pp.133–139.